

Real-Time Estimation of Thumb-Tip Forces using Surface Electromyogram for a Novel Human-Machine Interface

Wonil Park, Suncheol Kwon, and Jung Kim, *Member, IEEE*

Abstract— Due to difficulties in measurement of muscle activities and understanding a user's intention under different configurations, controlling machine forces using surface electromyogram (SEMG) is difficult in a human-machine interface (HMI). This study describes a novel HMI using Hill-based muscle model to control the isometric force of a robotic thumb that considers the importance of the thumb in hand function. In order to estimate force intensity, SEMG from the skin surface was measured and converted to muscle activation information. The activations of deep muscles were inferred from the ratios of muscle activations from earlier studies. The muscle length of each contributed muscle was obtained by using a motion capture system and musculo-skeletal modeling software packages. Once muscle forces were calculated, thumb-tip force was estimated based on a mapping model from the muscle force to thumb-tip force. The proposed method was evaluated in comparisons with a linear regression and artificial neural network (ANN) under four different thumb configurations to investigate the potential for estimations under conditions in which the thumb configuration changes.

I. INTRODUCTION

With the increasing development of machines which are driven by a user's movement intention such as prostheses and exoskeletons, the human-machine interface (HMI) has received a great deal of research attention. The HMI should provide an effective channel of clear communication between the user and the machine and also be intuitive to the user for natural usage. To satisfy these issues, surface electromyogram (SEMG) has become a popular approach for HMI because SEMG provides important muscle activation information of exerted forces; moreover, it can be measured noninvasively. Therefore, it can be possible to control machine intuitively with this signal.

Many researchers have investigated how to control the motion or force of machines for different body parts using SEMG [2-4]. Most studies of the hand have focused on controlling an artificial hand as a gripper or on classifying individual finger motions of a hand robot [5-6]. Few studies [7] but have investigated controlling the finger force using SEMG. Finger force is actually very important when people lift or hold objects. In particular, the thumb has the unique characteristic of opposability, and thumb-tip force allows the

hand to grasp objects [8]. Clinicians generally consider the thumb to be responsible for at least 50% of overall hand function [9]. Therefore, an advanced HMI in robotic hand applications should offer a way of controlling thumb-tip force using SEMG; additionally it should also have clear command flow even under different thumb configurations, when considering the configurations of the thumb in real life.

In order to control machine force corresponding to the user's intention with SEMG, several machine learning approaches are available, including a support vector machine (SVM) and an artificial neural network (ANN). In [7], SVM and ANN were used to estimate force from SEMG on finger parts. However, these approaches are known to have low performance outside of the specific tasks defined by the training and learning sets.

One alternative method for estimating force from SEMG under unspecific cases is the use of Hill-based muscle model, a phenomenological model of muscle contraction that many researchers have contributed to developing [10-11]. It can estimate force under general cases because it describes internal muscle mechanics. There have been much research to use the Hill-based muscle model to estimate muscle force [2, 4, 12-13]. Rosen et al. [13] showed that the Hill-based muscle model performs acceptably in general cases, while the ANN showed high performance only in specific sets.

This study describes an HMI that offers isometric thumb-tip force control of a partial hand robot using the Hill-based muscle model. The proposed HMI was tested under four different thumb configurations to investigate performance under conditions in which the thumb configuration changes, comparing the proposed method with other force estimation methods using linear regression and ANN.

II. METHODS

An overall block diagram of the proposed method is shown in Figure 1. Thumb-tip forces are estimated using muscle activation information and a biomechanical model. Recorded SEMG was converted to muscle activation, and the length of each contributing muscle was obtained by using a motion capture system (Motion Analysis Co., USA) and musculoskeletal modeling software (SIMM, Musculographics, USA). Once muscle forces were calculated, thumb-tip force was estimated based on a mapping model from the muscle force to thumb-tip force. Internal parameters in the estimation method were adjusted using a genetic algorithm. Finally, the calculated thumb-tip force was fed into the robotic thumb and the users could produce as much thumb-tip force as they intended to exert using SEMG. The

Won-Il Park is with LG Electronics, Seoul, Korea
Tel : +82-10-5775-9039; E-mail: park9039@kaist.ac.kr
Sun-Cheol Kwon is with Department of Mechanical Engineering, KAIST, Daejeon, Korea
Tel : +82-42-869-3271; E-mail: sun.kwon@kaist.ac.kr
Jung Kim is with Department of Mechanical Engineering, KAIST, Daejeon, Korea
Tel : +82-42-869-3231; E-mail: jungkim@kaist.ac.kr

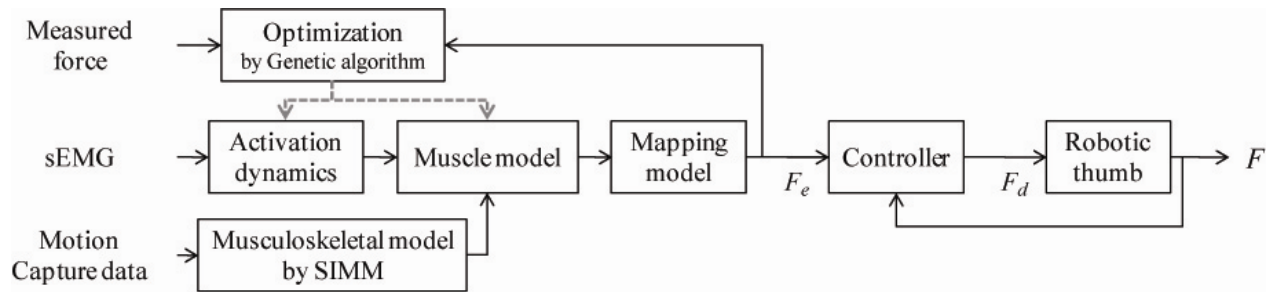


Fig. 1. Overall block diagram

force estimation algorithm was described in detail in our previous study [14].

2) There are nine muscles and three joints responsible for thumb motion [15]. They are *Adductor Pollicis* (AP), *Dorsal Interosseous* (DIO), *Flexors Pollicis Brevis* (FPB), *Flexors Pollicis Longus* (FPL), *Abductors Pollicis Longus* (APL), *Opponens Pollicis* (OPP), *Extensors Pollicis Longus* (EPL), *Abductors Pollicis Brevis* (APB) and *Extensors Pollicis Brevis* (EPB). Interactive anatomy software (ADAM Interactive Anatomy, A.D.A.M. Inc., USA), was used to find which of these muscles are located in the outermost layer. It was determined that five muscle activities can be observed from the surface: AP, FPB, APB, DIO and APL. Therefore, these muscles were chosen for collecting SEMG and the correct placement of the electrodes was verified by function muscle testing [16]. The reference electrode was attached on the *ulnar* bone of the elbow.

3) Muscle activation: The SEMG signals from the five surface muscles were recorded using bipolar surface electrodes (DE-2.1, Delsys, US). The signals were converted to muscle activation by a following signal processing technique. The signals were pre-amplified 1000 times and sampled at 1000Hz using a 16 bit A/D converting board (PCI-6034E, National Instruments, USA). The signal was then digitally processed using a) band-pass filter (10 - 470 Hz), b) DC offset, c) full wave rectification, d) moving average filter (200ms window and 100ms overlapping step), e) normalization with respect to the maximal isometric muscle activation levels of each muscle from manual muscle testing [17], f) nonlinear scaling to reflect nonlinearity in the EMG-to-activation relationship and g) activation level offset. Nonlinear scaling is defined by eq (1), where A determines the degree of nonlinearity and $a(t)$ is the processed EMG [12]. Activation level offset was performed because even if the hand was fully resting, there was a little activation offset. All the filters were Butterworth 5th order and the resultant activation level had a value between 0 and 1, where 0 indicates no muscle activation and 1 represents maximal muscle contraction.

A. Thumb-tip force estimation using the Hill-based muscle model

1) Muscle selection: The

$$a(t) = \frac{A^{u(t)} - 1}{A - 1} \quad (1)$$

In this study, SEMG signals were recorded from only five muscles due to anatomical limitations, even though nine muscles are responsible for exerting thumb-tip force. Several techniques, e.g. averaging SEMG of the adjacent muscles [12], have been introduced to obtain the non-observable SEMG. However, it is difficult to use these simple assumptions for a hand because the muscles are located deep inside the hand and they are too small. Therefore, we used the specific ratio of muscle activations between the muscles of the thumb to obtain activations of deep-layered muscles. In [18], all EMG levels of the thumb muscles were observed invasively using wire electrodes when the subject reached the maximal level of thumb-tip force at a key-pinching configuration that was equivalent to the hand configuration in the current study. The measured EMG amplitude was normalized to the highest value during a maximal voluntary contraction under manual muscle testing. In the present study, the activation ratio between muscles was assumed to be static while exerting force, because the relative activity of the contributing muscles did not change when modulating fingertip force magnitude across the voluntary range [19]. For more accurate estimation, the non-observable muscle activations were determined based on the similar functional muscle group; FPL and OPP were determined based on FPB and AP respectively. EPL and EPB's muscle activation was determined based on APL.

4) Muscle length identification: To calculate isometric muscle force, the length of the muscle length must be determined as well as the muscle activations because isometric muscle force changes depending on muscle length [10]. SIMM was used to estimate muscle length by averaging the muscle-tendon length from the motion-captured data. The generic model was scaled to a specific subject with the assumption that the subjects were of similar anthropometric proportions. Holzbaur *et al.* [20] created extrinsic muscles from the upper limb model in the software, and we created the intrinsic muscles (not included in the software) as a single

segment extending between the origin and insertion points [14]. Muscle origin and the insertion points of each muscle were defined as the centroids of muscle attachment areas based on anatomy software. Wrap objects are added on each joint to keep the muscle from penetrating the bone segment. Since the length from the origin to the insertion point in SIMM is the muscle-tendon length, muscle length can be calculated by subtracting the tendon length. In this study, the tendon was considered to be stiff because this element has been reported to be stiffer than the parallel component [21]. The fixed tendon length was obtained from the muscle-tendon length at 0 degree by using the relative ratio between the muscle fiber and tendon length.

5) Muscle model: The Hill-based muscle model is a simplified phenomenological model that describes muscle contraction and which allows muscle force to be estimated according to the processed neural activity, the change of the muscle length, and the contraction velocity [10]. The model represents an active muscle consisting of three elements: the contractile element (CE), the serial element (SE), and the parallel element (PE). The CE and PE represent an active muscle fiber and membrane outside the contractile elements. When the serial elastic element in cross-bridges of the CE is neglected because energy stored in the SE of cross-bridges is very small [22], the SE can be considered to be a tendon. When motor neurons stimulate a muscle to contract, the CE begins to shorten and the total muscle force is calculated by eq (2). The CE is the dominant component of the Hill-based model; under isometric conditions, the output force can be described by eq (3) where a is the muscle activation and scale the size of the active parabolic curve, f_l is the normalized force-length function and $F_{CE_{max}}$ is the maximal muscle force which is produced at maximal activation. The force-length equation is defined by (4) where L_{CE} is the length of the CE element, L_{CE_0} is the optimal fiber length at which the maximal muscle force is produced, and ϕ is a parameter affecting the variance of the Gaussian. More detailed equations of Hill-based muscle model force were described in our previous study [14] and in the literature [10-11].

$$F_{muscle} = F_{CE} + F_{PE} \quad (2)$$

$$F_{CE} = a \cdot f_l \cdot F_{CE_{max}} \quad (3)$$

$$f_l = e^{\left[-0.5 \left(\left(\frac{\Delta L_{CE}}{\Delta L_{CE_0}} - 1 \right) / \phi \right)^2 \right]} \quad (4)$$

6) Estimation of thumb-tip force: To obtain the thumb-tip force from muscle forces, a mapping model from muscle

forces to thumb-tip force was used. In our setup, the thumb-tip force vector was assumed to be only in the palmar direction. Therefore, the mapping model was based on the measured relationship between the input tendon tensions and the output thumb-tip force vectors in the palmar direction, according to the study by Pearlman *et al.* [1]. The magnitude of thumb-tip force in the palmar direction and the applied muscle force are shown in Table I. Thumb-tip force can be estimated by summing the palmar-directional forces by each muscle. Therefore, the total thumb-tip force can be calculated by (5).

$$F_{thumb-tip} = \sum_{i=1}^9 K_i F_{muscle_i} \quad (5)$$

where K indicates the mapping gain based on Table I, and subscript i indicates the i^{th} muscle. Among the nine thumb muscles, the force vectors of DIO were changed based on the physiologic cross-sectional area (PCSA) of the AP muscle because the subjects produced thumb-tip force with both the thumb and index finger, while only the thumb was used to produce force in the original experiments.

7) Muscle parameter optimization using Genetic Algorithm (GA): In the Hill-based model, there are internal parameters to describe muscle contraction that are important to adjust for the specific subject to give a realistic description of the muscle force exertion. The physical parameters ($\Delta L_{PE_{max}}$, L_{CE_0} , ϕ , S) are introduced to reflect inherent differences between subjects, whereas parameter A is calibrated depending on electrode placement and moisture of skin. However, these parameters are very difficult to measure due to anatomical and physiological variability. To find the internal parameters, a genetic algorithm (GA) was used in the absence of complete information by minimizing objective function. In the current study, optimization was performed with the genetic algorithm optimization toolbox (GAOT) in Matlab (Mathworks Inc., USA) [23] and the number of iterations was set to 20 empirically. In the algorithm, the chromosome was designed with 33 “genes” and five parameters for each of the nine thumb muscles were determined (A is calibrated only for measured muscle and ϕ has same value for all nine muscles). The parameters were then optimized by minimizing the root-mean-squared errors (RMSE) between the measured and estimated thumb-tip force.

Optimization was performed to reflect different physical conditions using only the data from 0-degree configuration of every set. The parameters obtained by the optimization were used to estimate the force in other thumb configurations, because the referred activation ratio [18] was obtained at 0 degree. Generally, it is reasonable to optimize parameters at one task because physical parameters and SEMG-related parameters do not changed as long as electrode placement remains [4].

TABLE I
MEASURED MUSCLE FORCES AND THUMB-TIP FORCES
IN PALMAR DIRECTION [1]

Muscle	Force	Muscle	Force	Muscle	Force
AP	14.4, 1.3	DIO	12.6, 3.51	FPB	12.6, 1.1
FPL	26.1, 5.6	APL	30, 0.1	OPP	18.3, -0.2
EPL	12.6, -0.9	APB	10.5, 0.5	EPB	7.8, -0.9

§ In force column, upper value and lower value means muscle force (N) and corresponding thumb-tip force (N), respectively.

B. Experimental protocol

Experiments were performed separately for off-line analysis and real-time estimation. In both off-line and real-time experiments, three healthy, right-handed males (age 26.6 ± 2.9) participated. None of the subjects had a history of upper extremity or other musculoskeletal complaints. Before experiments, initial recording at fully resting state of the hand and manual muscle testing were performed for all subjects. During this session, activation offset and maximal muscle activation were calculated for the nine muscles. The maximal muscle activation level was obtained by exerting maximal force against a palmar direction based on the muscle testing method [17].

The experiments for off-line analysis consisted of two parts: generic model scaling and thumb-tip force recording. After an initial recording session and manual muscle testing, subjects were asked to stand in the vicinity of motion capture cameras (six Eagle Digital Cameras and two Hawk Digital Cameras, Motion Analysis Co., USA) with 19 reflective markers placed on the subject's upper body and static motion-captured data for each subject during 3 seconds were recorded with 60 Hz sampling frequency. After recording, the captured data were fed into the SIMM and the generic model in the software was scaled to a specific subject based on the ratio of segment lengths. Once the generic model was scaled to a subject, the subject was seated on a chair and asked to exert thumb-tip force for 80 seconds following the guide force from the monitor. The guide force and current force level were represented as a bar graph. The guide force was composed of static (10, 20, 30 N) and dynamic levels by generating a sinusoidal function for 80 seconds. The upper limit of the guide force induced subjects to exert approximately 40% of the maximal pinching force with the assumption that the maximal thumb-tip force is 80 N. The one-axis force sensor (651AL, Maximum force 10kgf, KTOYO Inc., Korea) was mounted on aluminum posts which have four different angles; the angle between the force sensor plate and the ground was 0, 15, 30, and 45 degrees, as described in our previous study [14]. In the current experiments, each set consisting of the thumb-tip force recording from 0 to 45 degrees was repeated twice per subject. While the subject produced thumb-tip force, the force, SEMG and motion-captured data were recorded simultaneously. Reflective markers attached to the fingers during a static motion recording, excluding the thumb, were removed. The force measured by the sensor was acquired at 10Hz using a 16bit A/D converter (PCI-7354, National InstrumentsTM, USA). Then the force values were digitally

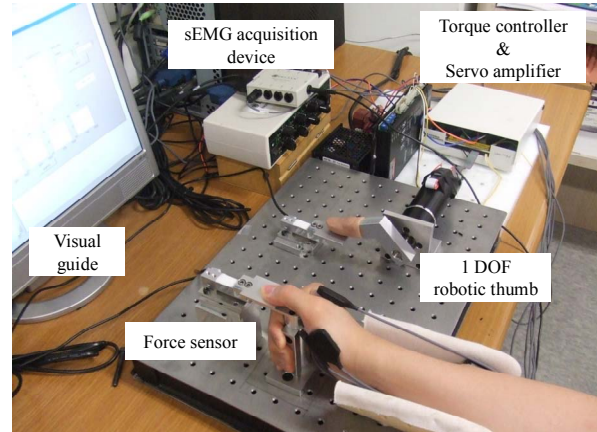


Fig. 2. Experimental setup for real-time estimation

processed with a low-pass filter (cutoff frequency 3Hz). A 2-min recovery period was given between contractions. Additionally, subjects had a 5-min break after completing each set.

C. Evaluation of Experiments

To evaluate the performance of the proposed method, the force was estimated using linear regression and ANN. The muscle activation for linear regression was calculated using integrated EMG (IEMG). In the present study, the AP muscle was selected for calculating the IEMG signal because the AP is one of the main agonist muscles involved in thumb motion [18]. The SEMG signal from the AP was integrated over periods of 200ms and overlapped with 100ms step. In addition to the linear regression method, two ANN models were developed to investigate the influence of training data on estimation performance; one was trained only with 0-degree data, while the other was trained with the data from all configurations. Each ANN included one hidden layer and fifteen hidden nodes and was trained using the Levenberg-Marquart algorithm with Matlab. The optimization process for the proposed model, linear regression, and ANN were performed to adjust the internal parameters and train the neural network. In off-line analysis, optimization was done using the 0-degree data or data from all configurations and then used to estimate the force in the same set.

In the real-time force estimation experiments, the initial recording and manual muscle testing were performed again and the additional thumb-tip force data from four configurations not included in the regular set were used for optimization because the placement of electrodes was different from off-line experiments. Once the parameters were calibrated, two sets of experiments were performed during 80 seconds. The experimental setup for real-time estimation is illustrated in Figure 2. While subjects exert thumb-tip force under four configurations, the force was estimated in real time with four methods simultaneously, whereas the robotic thumb was controlled only with the signal from the proposed method. The control board (PCI-7354, National InstrumentTM, USA) was used to rotate a DC motor (RE-40, Maxon motor, Switzerland) which generated current signal output which was directly proportional to the motor

torque. The force control algorithm using a PD controller is shown in (6).

$$F_d = F_e + K_P(F_e - F) + K_D(\dot{F}_e - \dot{F}) \quad (6)$$

where F_e is the estimated force from the proposed model, F is the current force of the slave part, and F_d is the control input. Feedback gain K_P and K_D were fixed to 0.05 and 0.008 respectively through empirical tuning, and motor command updates were sent to the controller every 100ms. The Matlab data acquisition toolbox and external interface link were used to control the machine simultaneously with the acquisition of SEMG signals.

III. RESULTS AND DISCUSSION

The off-line and real-time results are shown in Table II and III. The real-time results presented in these tables were based on the estimated force, not the measured force from the robotic thumb. The performance was quantified using two criteria: the RMSE and the correlation coefficient (CORR). The Hill-based muscle model (HBMM), linear regression (LR), ANN_1 trained with 0-degree data, and ANN_2 trained with all configurations data were then compared. The measured force from the robotic thumb is plotted in Figure 3. The gray solid line, black solid line and black dotted line indicate the measured force from the subject part, the predicted force by the proposed method and the measured force from the robotic thumb respectively.

In the off-line analysis results, HBMM showed better performance than the LR method. LR showed acceptable error in 0 and 15 degrees, but the performance decreased as the configurations changed. ANN_1 showed the highest performance at 0 degree, but the performance rapidly decreased as the configurations changed. On the other hand, HBMM showed a smaller error and a higher correlation than LR or ANN_1 even under other configurations. These results are identical to those in [13] where ANN showed high performance in a training set, while HBMM showed acceptable error in general cases. It is also noted that the performance of ANN_1 was better than ANN_2 at 0 degree even if ANN_2 was trained with data from all configurations, while the overall performance of ANN_2 was the highest from all angles

Real-time estimation showed that the estimation error increased in every method compared to the off-line analysis results, but HBMM has the lowest increasing rate of error. From this, it can be concluded that the physical model-based estimation method is more robust to real-time environments than LR or ANN. From the Table III, the proposed method has better performance than LR and ANN_1 in the real-time experiments as well. The predictions by ANN_1 and ANN_2 were somewhat hampered because the input signals in the real-time experiments were different from the data used in the training session. The error of ANN_1 and ANN_2 at 0 degree is relatively larger than other configurations, because over-fitting problems occurred. The overall performance of ANN_2 was still better than that of the other methods in

TABLE III
OFF-LINE ANALYSIS RESULTS

Degree	HBMM		LR	
	RMSE (N)	CORR	RMSE (N)	CORR
0	1.87	0.98	3.43	0.97
15	3.30	0.98	3.49	0.97
30	3.45	0.98	7.32	0.97
45	4.43	0.98	9.63	0.97
Degree	ANN 1		ANN 2	
	RMSE (N)	CORR	RMSE (N)	CORR
0	1.16	0.99	1.62	0.99
15	4.87	0.90	1.44	0.99
30	7.48	0.78	1.33	0.99
45	8.53	0.78	1.28	0.99

TABLE IV
REAL-TIME ESTIMATION RESULTS

Degree	HBMM		LR	
	RMSE (N)	CORR	RMSE (N)	CORR
0	5.28	0.97	7.97	0.92
15	4.10	0.99	11.18	0.97
30	4.71	0.98	16.04	0.97
45	3.87	0.98	16.12	0.96
Degree	ANN 1		ANN 2	
	RMSE (N)	CORR	RMSE (N)	CORR
0	9.99	0.64	6.15	0.88
15	7.58	0.87	3.98	0.96
30	8.50	0.87	3.41	0.97
45	10.69	0.73	3.53	0.96

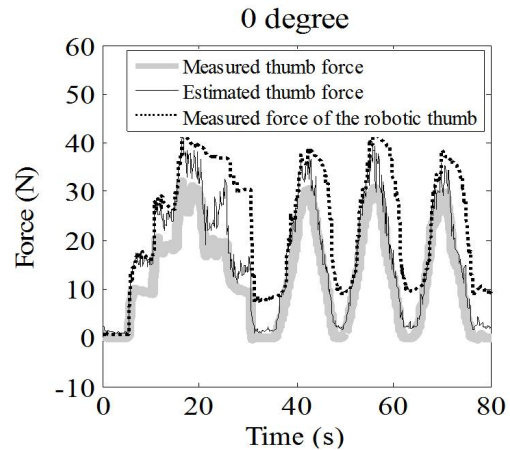


Fig. 3. Force trajectories of subject 1, set #1 in real-time estimation

real-time experiments. LR showed the biggest error in all conditions except 0 degree. HBMM had a high correlation value in every experimental case, which is very important because high correlation means that the force intension of the subject was conveyed to the robot well. The LR method showed poor performance in most experimental cases, because LR only depends on the muscle signals from one muscle, and the estimation performance is very sensitive to the condition of the muscles selected.

IV. CONCLUDING REMARKS

The present study describes an HMI offering isometric thumb-tip force control of a thumb robot using the Hill-based muscle model. The proposed HMI was tested under four different thumb configurations and was compared with other

force estimation methods such as a linear regression and ANN for evaluations. The proposed method based on the physical model showed acceptable errors in every experimental case and had high correlation value while the performance of linear regression and ANN- trained was reduced as the configuration changed. ANN trained with the data from all configurations showed the best overall performance, but it is necessary to gather data from every configuration which the thumb can make in order to have good performance in every situation.

The main contribution of this study is the first physical muscle model-based thumb-tip force estimation. It was demonstrated to be an efficient method capable of estimating force in other configurations even with parameters which are calibrated at a specific angle, and it is more robust to real-time environments. Our interface can also be extended to other muscles for the other four fingers. Therefore, it is concluded that the proposed HMI is useful for force control in partial finger prostheses.

ACKNOWLEDGMENT

This work was supported by the Korea Science and Engineering Foundation (KOSEF) grant funded by the Korea government (MOST) (No. R01-2007-000-11659 -0).

REFERENCES

- [1] J. Pearlman, S. Roach, and F. Valero-Cuevas, "The fundamental thumb-tip force vectors produced by the muscles of the thumb," *Journal of Orthopaedic Research*, vol. 22, pp. 306-312, 2004.
- [2] C. Fleischer and G. Hommel, "A Human--Exoskeleton Interface Utilizing Electromyography," *IEEE Transactions on Robotics*, vol. 24, pp. 872-882, 2008.
- [3] O. Fukuda, T. Tsuji, M. Kaneko, and A. Otsuka, "A human-assisting manipulator teleoperated by EMG signals and arm motions," *IEEE Transactions on Robotics and Automation*, vol. 19, pp. 210-222, 2003.
- [4] E. E. Cavallaro, J. Rosen, J. C. Perry, and S. Burns, "Real-Time Myoprocessors for a Neural Controlled Powered Exoskeleton Arm," *IEEE Transactions on Biomedical Engineering*, vol. 53, pp. 2387-2396, 2006.
- [5] F. Tenore, A. Ramos, A. Fahmy, S. Acharya, R. Etienne-Cummings, and N. V. Thakor, "Towards the Control of Individual Fingers of a Prosthetic Hand Using Surface EMG Signals," in *Proceedings of the 29th Annual International Conference of the IEEE Engineering in Medicine and Biology Society*, pp. 6145-6148, 2007.
- [6] K. Nagata, K. Ando, K. Magatani, and M. Yamada, "Development of the hand motion recognition system based on surface EMG using suitable measurement channels for pattern recognition," in *Proceedings of the 29th Annual International Conference of the IEEE Engineering in Medicine and Biology Society*, pp. 5214-5217, 2007.
- [7] C. Castellini and P. van der Smagt, "Surface EMG in advanced hand prosthetics," *Biological Cybernetics*, vol. 100, pp. 35-47, 2009.
- [8] F. J. Bejjani and J. M. F. Landsmeer, "Biomechanics of the hand," *Basic biomechanics of the musculoskeletal system*, vol. 2, pp. 275-304.
- [9] J. C. Colditz, "Anatomic considerations for splinting the thumb," *Rehabilitation of the hand and upper extremity*. St. Louis: Mosby, pp. 1858-75, 2005.
- [10] J. M. Winters, "Hill-based muscle models: a systems engineering perspective," *Multiple Muscle Systems: Biomechanics and Movement Organization*, JM Winters and SL-Y Woo eds, Springer-Verlag, 1990.
- [11] F. E. Zajac, "Muscle and tendon: properties, models, scaling, and application to biomechanics and motor control," *Crit Rev Biomed Eng*, vol. 17, pp. 359-411, 1989.
- [12] D. G. Lloyd and T. F. Besier, "An EMG-driven musculoskeletal model for estimation of the human knee joint moments across varied tasks," *Journal of Biomechanics*, vol. 36, pp. 765-776, 2003.
- [13] J. Rosen, M. B. Fuchs, and M. Arcan, "Performances of Hill-Type and Neural Network Muscle Models: Toward a Myosignal-Based Exoskeleton," *Computers and Biomedical Research*, vol. 32, pp. 415-439, 1999.
- [14] W. Park, S. Kwon, H. Lee, and J. Kim, "Thumb-tip force estimation from SEMG and a musculoskeletal model for real-time finger prosthesis," in *Proceedings of IEEE International Conference on Rehabilitation Robotics*, pp. 305-310, 2009.
- [15] E. Y. Chao, *Biomechanics of the Hand: A Basic Research Study*: World Scientific Pub Co Inc, 1989.
- [16] A. A. Leis and V. C. Trapani, *Atlas of electromyography*: Oxford University Press New York, 2000.
- [17] N. C. Cutter and C. G. Kevorkian, *Handbook of manual muscle testing*: McGraw-Hill, Health Professions Division, New York, 1999.
- [18] M. E. Johanson, F. J. Valero-Cuevas, and V. R. Hentz, "Activation patterns of the thumb muscles during stable and unstable pinch tasks," *Journal of Hand Surgery*, vol. 26, pp. 698-705, 2001.
- [19] F. J. Valero-Cuevas, "Predictive modulation of muscle coordination pattern magnitude scales fingertip force magnitude over the voluntary range," *Journal of Neurophysiology*, vol. 83, pp. 1469-1479, 2000.
- [20] K. R. S. Holzbaur, W. M. Murray, and S. L. Delp, "A Model of the Upper Extremity for Simulating Musculoskeletal Surgery and Analyzing Neuromuscular Control," *Annals of Biomedical Engineering*, vol. 33, pp. 829-840, 2005.
- [21] P. Bawa and R. B. Stein, "Frequency response of human soleus muscle," *Journal of Neurophysiology*, vol. 39, pp. 788-793, 1976.
- [22] S. L. Delp, J. P. Loan, M. G. Hoy, F. E. Zajac, E. L. Topp, J. M. Rosen, V. A. M. Center, and P. Alto, "An interactive graphics-based model of the lower extremity to study orthopaedic surgical procedures," *IEEE Transactions on Biomedical Engineering*, vol. 37, pp. 757-767, 1990.
- [23] "The Genetic Algorithm Optimization Toolbox (GAOT)." www.ise.ncsu.edu/mirage/GAToolBox/gaot/, [Online].